JACS Au
AN OPEN ACCESS JOURNAL OF THE AMERICAN CHEMICAL SOCIETY

pubs.acs.org/jacsau
Article

Engineering Bifunctional Galactokinase/Uridyltransferase Chimera for Enhanced UDP-D-Xylose Production

Published as part of JACS Au virtual special issue "Biocatalysis in Asia and Pacific".

Jin-Da Zhuang,† Jin-Min Shi,† Chen-Cheng Hong, Ting-Ting Wu, Li Liu,* and Josef Voglmeir*

Cite This: JACS Au 2024, 4, 2557−2563
Read Online

ACCESS | Metrics & More | Article Recommendations | Supporting Information

ABSTRACT: The biotechnological production of uridine diphosphate-D-xylose (UDP-D-xylose), the glycosyl donor in enzymatic for D-xylose, is an important precursor for advancing glycoengineering research on biopharmaceuticals such as heparin and glycosaminoglycans. Leveraging a recently discovered UDP-xylose salvage pathway, we have engineered a series of bifunctional chimeric biocatalysts derived from *Solitalea canadensis* galactokinase/uridyltransferase, facilitating the conversion of D-xylose to UDP-D-xylose. This study elucidates the novel assembly of eight fusion protein constructs, differing in domain orientations and linker peptide lengths, to investigate their functional expression in *Escherichia coli*, resulting in the synthesis of the first bifunctional enzyme that orchestrates a direct transformation from D-xylose to UDP-D-xylose. Fusion constructs with a NH_2-GSGGGSGHM-COOH peptide linker demonstrated the highest expression and catalytic tenacity. For the highest catalytic conversion from D-xylose to UDP-D-xylose, we established an optimum pH of 7.0 and a temperature optimum of 30 °C, with an optimal fusion enzyme concentration of 3.3 mg/mL for large-scale UDP-D-xylose production. Insights into ATP and ADP inhibition further helped to optimize the reaction conditions. Testing various ratios of unfused galactokinase and uridyltransferase biocatalysts for UDP-xylose synthesis from D-xylose revealed that a 1:1 ratio was optimal. The K_{cat}/K_m value for the NH_2-GSGGGSGHM-COOH peptide linker showed a 10% improvement compared with the unfused counterparts. The strategic design of these fusion enzymes efficiently routes for the convenient and efficient biocatalytic synthesis of xylosides in biotechnological and pharmaceutical applications.

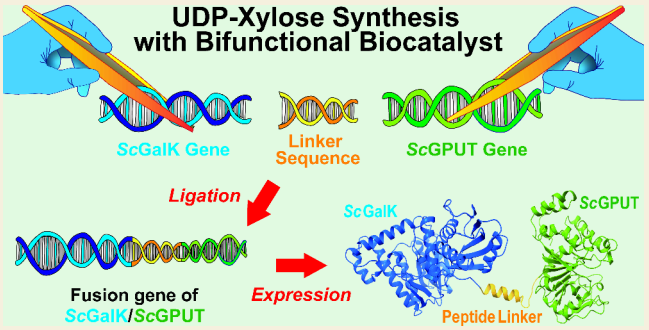

KEYWORDS: *UDP-D-xylose production, bifunctional enzyme, fusion proteins, synthetic biology, glycoengineering, galactokinase/uridyltransferase chimera, peptide linkers*

INTRODUCTION

Engineering new biocatalytic pathways to synthesize complex biomolecules is a fundamental aspect of synthetic biology. Among these biomolecules, UDP-D-xylose is an indispensable glycosyl donor for the assembly of xylose-containing glycosaminoglycans such as heparin and chondroitin sulfate. These glycoconjugates are essential in numerous biological processes and possess broad therapeutic applications.[1,2] Current methods to procure such biomolecules rely heavily on extraction from natural sources, which may raise concerns regarding sustainability, safety, and scalability. Therefore, establishing a straightforward and scalable synthesis for UDP-D-xylose could transform glycosaminoglycan manufacturing, shifting from the constraints of biological extraction to the adaptability of modular synthetic biocatalytic pathways.[3−5]

The traditional de novo biosynthesis of UDP-D-xylose starts from D-glucose and can be achieved by an enzymatic cascade consisting of four biocatalysts (Supplementary Figure S1): In the first step, D-glucose is phosphorylated by a hexokinase using ATP, yielding glucose 6-phosphate, which is then isomerized to glucose 1-phosphate by phosphoglucomutase.[6] This product is then converted by glucose-1-phosphate uridyltransferase to UDP-D-glucose, which is subsequently oxidized by UDP-glucose 6-dehydrogenase to form UDP-glucuronic acid.[7,8] The final decarboxylation step which yields UDP-xylose is mediated by UDP-glucuronate decarboxylase.[9,10] By contrast, a recently elucidated UDP-D-xylose salvage pathway in certain bacteria begins directly with the activation of xylose instead of glucose. A substrate-promiscuous galactokinase first phosphorylates xylose in the anomeric position, forming D-xylose 1-phosphate, which then is

Received: March 31, 2024
Revised: June 11, 2024
Accepted: June 12, 2024
Published: June 20, 2024

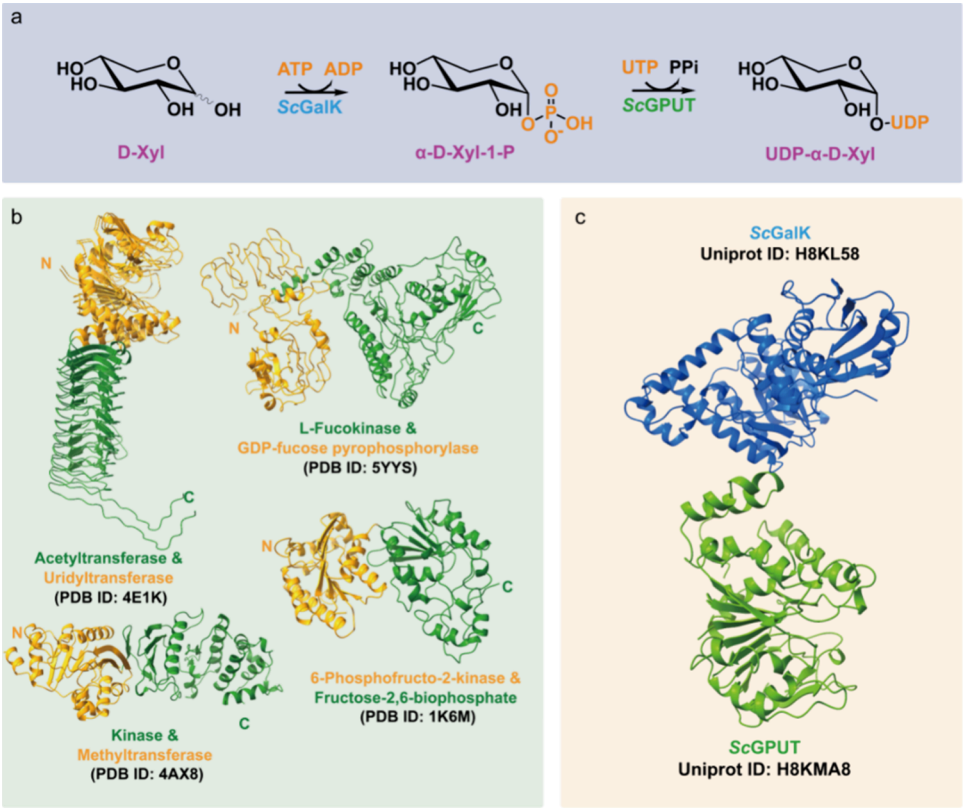

Figure 1. (a) Salvage pathway for UDP-xylose biosynthesis from xylose by *Sc*GalK/*Sc*GPUT. (b) Examples of bifunctional enzyme fusions in nature. (c) Model structure of fused *Sc*GalK and *Sc*GPUT.

conjugated with UTP by an equally versatile glucose-1-phosphate uridyltransferase to directly yield UDP-D-xylose.[10] This alternative route reduces the number of required enzymatic reactions to only two steps and eliminates the need for cofactor NAD^+ while utilizing only ATP and UTP. Therefore, this salvage pathway presents a more efficient and cost-effective approach to the synthesis of UDP-D-xylose (Figure 1a).

Our research direction has been influenced by the understanding that the production of UDP-D-xylose necessitates only two distinct enzymes. Examples of bifunctional proteins are common in nature and incorporate two separate catalytic activities within a single protein structure (Figure 1b). They efficiently catalyze consecutive reactions, thereby facilitating the transition from one reaction product to another. For instance, the enzyme L-fucokinase/GDP-L-fucose pyrophosphorylase catalyzed both phosphorylation and pyrophosphorylase reactions to transform fucose into GDP-fucose in one continuous process.[11] Similarly, the enzyme pair glucurono-kinase/UDP-glucuronate pyrophosphorylase efficiently converts glucuronate to UDP-glucuronic acid.[12] Extending this concept to synthetic biology, fusion proteins have been successfully engineered, as exemplified by the coupling of *N*-acetylhexosamine 1-kinase with a truncated uridyltransferase to yield UDP-GlcNAc from GlcNAc.[13] Such engineered fusion enzymes not only underscore their potential for large-scale production but also highlight their capacity for synthesizing analogs and establishing novel metabolic pathways to support glycosylation reactions. Crucial to the efficacy of these chimeric proteins is the correct specification of the linker peptides connecting the enzyme units—their type, length, and amino acid composition being imperative factors in maintaining both activity and stability.[14,15]

Nevertheless, to date, no single fusion protein or naturally occurring bifunctional enzyme has been described for the direct conversion of D-xylose to UDP-D-xylose (Figure 1c). In the present study, we combined two assembly orientations and four linker peptides with different lengths and compared the catalytic performance of the eight resulting chimeric fusion enzymes. These constructs were then assessed for their activity to determine the most effective bifunctional enzyme configuration for UDP-D-xylose synthesis.

The orientation and composition of the peptide linkers greatly influenced the catalytic efficiency of our chimeric enzymes. Constructs such as *Sc*GalK-GSGGGSGHM-*Sc*GPUT (Linker 4) and *Sc*GPUT-GSGGGSGHM-*Sc*GalK (Linker 8) demonstrated significant variations in activity due to differences in domain orientation and linker length. Linkers rich in glycine and serine enhanced expression and solubility, thereby increasing enzyme activity. Constructs with the pyrophosphorylase domain at the N-terminus generally showed higher product formation; however, an appropriate linker design can mitigate orientation disadvantages. These findings underscore the necessity of meticulous linker design in optimizing the catalytic performance of bifunctional chimeric proteins. While positioning the pyrophosphorylase domain at the N-terminus generally showed higher product formation, our data indicate that certain configurations with the kinase domain at the N-terminus, notably Linker 4, also resulted in high product formation. These findings show the necessity of a careful linker to achieve the optimum catalytic performance of bifunctional chimeric proteins.

https://doi.org/10.1021/jacsau.4c00288
JACS Au 2024, 4, 2557−2563

RESULTS AND DISCUSSION

Expression, Purification, and Activity Evaluation of Bifunctional Enzyme Constructs

Expression, purification, and activity testing of various constructs led to the generation of eight recombinant vectors, each incorporating different linker peptides—NH_2-HM-COOH, NH_2-GSGHM-COOH, NH_2-GGGGSHM-COOH, and NH_2-GSGGGSGHM-COOH—and oriented in two fusion configurations, one with *Solitalea canadensis* galactokinase (*Sc*GalK) on the *N*-terminus (*Sc*GalK-linker-*Sc*GPUT), and one with *Solitalea canadensis* uridyltransferase (*Sc*GPUT) on the N-terminus (*Sc*GPUT-linker-*Sc*GalK, Figure 2). Linkers

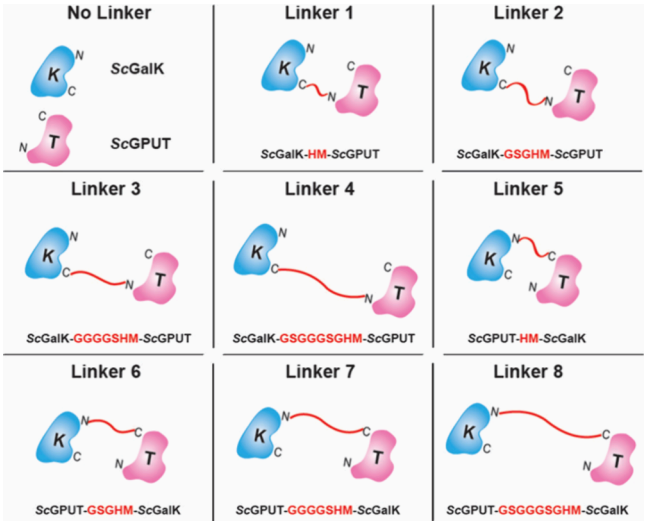

Figure 2. Overview of constructing the recombinant *Sc*GalK/*Sc*GPUT fusion proteins using different linkers.

are generally rich in small or polar amino acids such as glycine and serine to provide good flexibility and solubility.[16] Therefore, glycine and serine were used as linkers in various fusion proteins,[17] while histidine and methionine residues were derived from *Sc*GalK or *Sc*GPUT. The choice of linker length is supported by Argos's work, which indicates that natural linkers average 6.5 residues, predominantly consisting of Gly and Ser for optimal flexibility and solubility.[18]

These constructs were expressed in BL21 (DE3) cells, yielding the respective target protein with molecular weights of approximately 70 kDa. While proteins with peptide linker 1 were primarily insoluble, the remaining fusion enzymes were expressed in soluble form and subsequently purified using nickel-affinity chromatography, as confirmed by distinct bands observed on SDS-PAGE (Supplementary Figure S2). Observed differences in expression levels were influenced by both the peptide linker sequence and the orientation of the fusion, with the longest linker peptide (NH_2-GSGGGSGHM-COOH) enhancing expression in both subunit orientations. However, obtaining pure recombinant protein proved more challenging for the *Sc*GPUT-linker-*Sc*GalK orientation (Figures 3a and S3).

Activity assays for the fusion enzymes were conducted in the presence of ATP and UTP, which assessed the biocatalytic transformation of D-xylose to UDP-xylose (Figure 3b). Techniques employed included thin-layer chromatography (TLC) (Figures 3c and S4a) and liquid chromatography-electrospray ionization-mass spectrometry (LC-ESI-MS) (Figure 3d,e), which confirmed that, except for constructs containing peptide linkers 1 and 7, all enzymes successfully synthesized UDP-xylose. In contrast, similar assays measuring the conversion of D-xylose-1-phosphate to UDP-xylose (Figures 3f and S4b) indicated that all but the peptide linker 7 constructs were effective.

These results suggest that the differences observed in Figure 3c,f might be due to the distinct roles of the phosphorylated intermediates and their accessibility in the reaction. Specifically, the spatial orientation imposed by different peptide linkers could influence the efficiency of the initial phosphorylation step catalyzed by the kinase subunit. For instance, constructs with peptide linkers 1 and 7 showed reduced activity in the conversion of D-xylose (Figure 3c), which we hypothesize is due to suboptimal spatial arrangement affecting the kinase subunit's access to D-xylose. Conversely, the conversion of D-xylose-1-phosphate was less affected by linker variability, except for linker 7, suggesting that once the sugar is phosphorylated, additional constraints impact productivity.

Typically, positioning the pyrophosphorylase domain at the N-terminus appears to be more favorable for product formation. This orientation of subunits can also be observed with previously reported natural and synthetically constructed fucose and glucoronate salvage enzymes, which typically house a kinase domain at the C-terminus and a pyrophosphorylase at the N-terminus.[11,12] While positioning the pyrophosphorylase domain at the N-terminus generally showed higher product formation, our data indicate that certain configurations with the kinase domain at the N-terminus, notably Linker 4, also resulted in high product formation. These findings show the necessity of a careful linker design to achieve the optimum catalytic performance of bifunctional chimeric proteins.

Biocatalytic Evaluation

SDS-PAGE analysis and activity tests were used to identify fusion enzymes that demonstrated soluble expression and functional catalytic activity. Specifically, constructs containing peptide linkers 3, 4, 5, 6, and 8 showed robust expression and catalytic activities. A 48 h time-course analysis using TLC and LC-ESI-MS was employed to monitor the conversion of D-xylose to UDP-D-xylose by these constructs (Figures 4a and S4), revealing that the formation of UDP-D-xylose product formation was observed within 8 h of incubation time. UDP-D-xylose formation progressively increased with time, and after 48 h, the reactions catalyzed by the enzymes with peptide linkers 4 and 8 yielded the highest levels of UDP-D-xylose (up to approximately 100 and 89% conversion based on xylose), suggesting that the extended length of peptide linker NH_2-GSGGGGSGHM-COOH facilitated a higher activity regardless of the fusion configuration.

Optimal catalytic conditions for the bifunctional fusion enzymes were determined to be at pH 7.0 and 30 °C (Figures 4b,c and S7), mirroring the favorable reaction conditions for the individual subunit *Sc*GalK, which was previously reported to work best at pH 7.0 and 30 °C.[10] TLC analysis was also utilized to ascertain the optimal enzyme concentration for the synthesis of UDP-D-xylose (Figures 4e and S6). For an optimal balance of cost-effectiveness and efficiency, a protein concentration of 3.3 mg/mL was identified as suitable for the large-scale production of UDP-D-xylose. Although these experiments were not performed in the present study, this concentration is based on methodologies described in the recent literature,[19] which suggests the feasibility of producing

https://doi.org/10.1021/jacsau.4c00288
JACS Au 2024, 4, 2557−2563

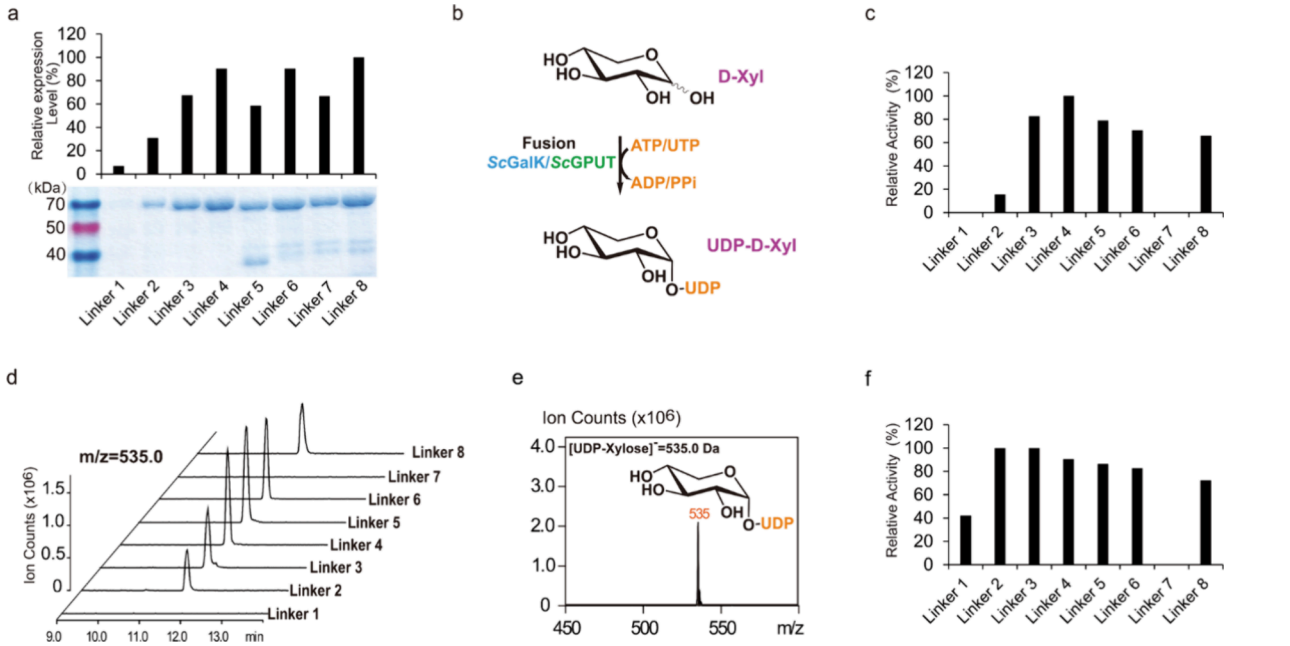

Figure 3. Expression, purification, and activity assessment of the various constructs. (a) SDS-PAGE analysis of purified recombinant fusion enzymes highlighted variations in linker peptides. (b) Enzymatic conversion of D-xylose to UDP-xylose by *Sc*GalK/*Sc*GPUT fusion enzymes. (c) TLC analysis results of the *Sc*GalK/*Sc*GPUT enzymes reacting with D-xylose. The conversion rate of linker 8 mentioned in the text (89%) is based on standardized conditions to match the enzyme concentration across different linkers. (d) LC-ESI-MS profile confirming the presence of UDP-xylose in reaction mixtures containing *Sc*GalK/*Sc*GPUT fusion enzymes. (e) Mass spectrum at a retention time of 11.6 min, indicative of UDP-xylose production. (f) TLC separation of products from the reaction of *Sc*GalK/*Sc*GPUT enzymes with D-xylose-1-phosphate.

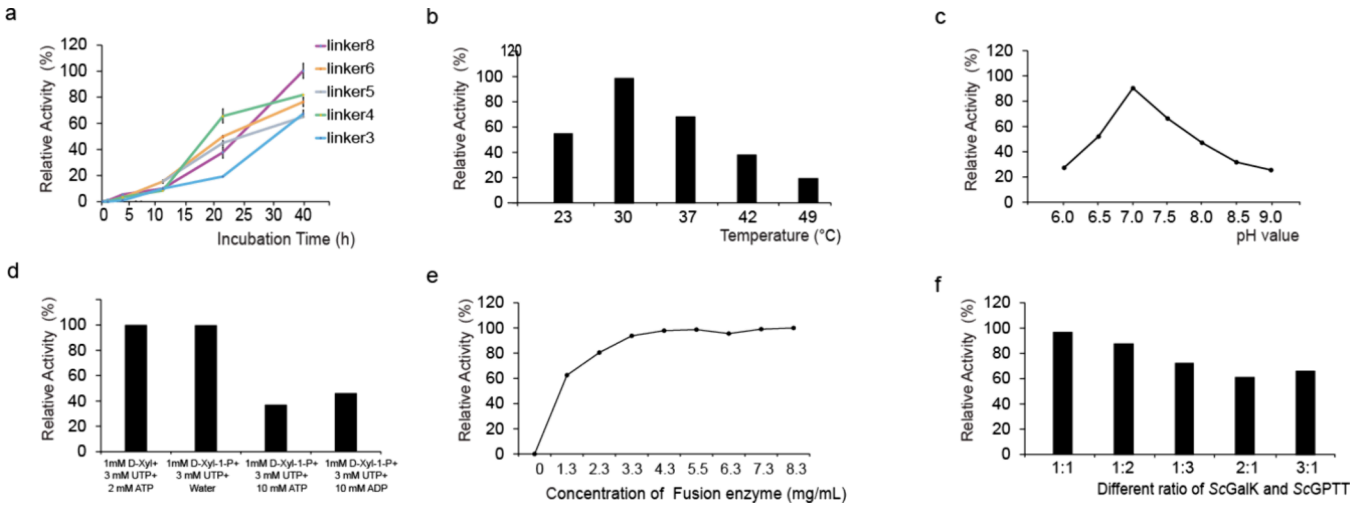

Figure 4. Biocatalytic evaluation of the bifunctional fusion enzymes. (a) 40 h time-course LC-ESI-MS reaction profiling for D-xylose conversion. (b) Optimal pH for the enzyme's activity, derived from TLC analysis. (c) Determination of the enzyme's optimum operating temperature. (d) TLC analysis displaying inhibition by ATP and ADP. (e) TLC results were used for identifying the optimal enzyme concentration for UDP-D-xylose enzymatic synthesis. (f) Determination of the enzymes' optimum operating ratios of *Sc*GalK/*Sc*GPUT.

UDP-xylose on a gram- to multigram-scale using a laboratory setup that incorporates shaking bottle fermentations for recombinant protein production. This method proves to be competitive with processes that use whole-cell biocatalysts for production, showcasing the potential for economical scalability.[19] Moreover, the assay identified that high concentrations (10 mM) of ATP and ADP serve as inhibitors of the catalytic activity of *Sc*GPUT, reducing the conversion rate of xylose-1-phosphate to UDP-xylose by over 50% (Figure 4d). Similar observations were made for other nucleotide-utilizing enzymes, such as kinases or pyrophosphorylases, where inhibition by ATP and its hydrolysis product ADP is well-documented.[20] In the case of ADP specifically, its accumulation as a byproduct can competitively hinder the binding of ATP, thus diminishing the enzyme's activity.[21] This inhibitory effect of ADP on the fusion enzyme's activity should therefore be optimized to minimize the reduction in reaction rates for UDP-xylose synthesis. To evaluate the best molar ratio of *Sc*GPUT to *Sc*GalK, various ratios of the unfused enzymes were tested for the synthesis of UDP-xylose from D-xylose. Figure 4f shows that the 1:1 ratio outperformed the other tested ratios, confirming its effectiveness. However, alternative

https://doi.org/10.1021/jacsau.4c00288
JACS Au 2024, 4, 2557−2563

strategies, like sugar nucleotide regeneration beads (Superbeads),[22] could be valuable for other optimal enzyme ratios. Superbeads allow coimmobilization of enzymes at tailored ratios, potentially enhancing catalytic efficiency by fine-tuning the proportion of the biocatalyst, thereby improving practical application and enzyme economy. To compare fusion *Sc*GPUT/*Sc*GalK with unfusion *Sc*GPUT/*Sc*GalK, kinetic analyses are shown in Supplementary Table S2. The K_m value of linker 8 for D-xylose to UDP-D-xylose was 0.9 ± 0.4 mM, V_{max} was 99 ± 12 μM h^{-1}, the k_{cat} value was 3.0 × 10^{-12} min^{-1}, and K_m/k_{cat} was 3.2 × 10^{-12}. The K_m/k_{cat} value of unfused *Sc*GPUT and *Sc*GalK was 2.9 × 10^{-12}. This indicated that the catalytic efficiency of NH_2-GSGGGSGHM-COOH peptide linker compared with unfused *Sc*GPUT and *Sc*GalK improved by 10%.

CONCLUSIONS

In this study, we engineered bifunctional fusion enzymes by combining two enzymes from the soil bacterium *Solitalea canadensis* that exhibit promiscuity toward D-xylose. This feat marks the first successful attempt to integrate the activities of these enzymes. The evaluated fusion enzymes present a promising biocatalytic tool for the cost-effective and efficient production of UDP-D-xylose and xylose-containing conjugates. Its development underscores the potential of such chimeric proteins to revolutionize the production of essential glycosyl donors, providing a sustainable alternative to traditional extraction methods for biopharmaceutical applications. The *Sc*GalK/*Sc*GPUT fusion enzyme, with its bifunctional biocatalytic capabilities, is well-suited for large-scale synthesis of UDP-D-xylose as well as for the production of various xylose-based bioproducts. Its application in industrial settings promises to enhance the efficiency and output of biochemical manufacturing.

EXPERIMENTAL PROCEDURES

Construction of Fusion Genes

For the cloning of bifunctional fusion constructs, genes encoding *Sc*GalK and *Sc*GPUT were cleaved from their pET30a vectors (Merck) using Nde*I* and Xho*I* endonucleases. Subsequently, these segments were inserted into pET28a vectors (Merck) already digested with the corresponding restriction overhangs. The amplicons, representing the full-length open reading frames of *Sc*GalK and *Sc*GPUT (UniProt identifiers H8KL58 and H8KMA8), were engineered to include a series of different linker peptides. The DNA sequences for these constructs, detailed in Supplementary Table S1, were amplified employing a polymerase chain reaction (PCR) facilitated by Taq DNA polymerase (Takara Premix). The resulting PCR products were then cloned directly into pGEM-T easy vectors (Promega).

After the transformation and plasmid recovery from *E. coli* transformants, the sequences encoding for *Sc*GalK and *Sc*GPUT, now featuring various linker peptides, were released using Nde*I* and Nco*I* restriction enzymes. These fragments were ligated into pET28a vectors already containing DNA sequences encoding for either *Sc*GalK or *Sc*GPUT and similarly pretreated with the analogous restriction enzymes. This approach resulted in the assembly of a series of bifunctional fusion enzyme expression vectors. Each of these constructs was engineered to display a C-terminal hexahistidine tag to facilitate subsequent purification steps.

Expression and Purification of Bifunctional Fusion Enzymes

For the production of *Sc*GalK/*Sc*GPUT fusion proteins, *E. coli* BL21 (DE3) cells were transformed with the pET28a fusion constructs and propagated in 400 mL cultures under shaking. These cultures were incubated for 20 h at a suboptimal temperature of 18 °C to enhance proper folding and solubility of the proteins. Cells were harvested using centrifugation at 4000*g* for 10 min at 4 °C. The pelleted cells were then resuspended in 10 mL of a cell lysis buffer (comprising 100 mM NaCl, 50 mM Tris−HCl, 1% (v/v) Triton X-100, and 1 mM phenylmethylsulfonyl fluoride (PMSF), pH 8.0) and subjected to cell disruption by sonication for a duration of 20 min.

Following the cell lysis, bacterial debris was sedimented by centrifugation at 20,000*g* for 20 min at 4 °C. The clarified supernatant containing soluble fusion proteins was applied to a Ni-NTA affinity column (Qiagen, 2 mL bed volume). A washing step was conducted using 20 mL of wash buffer (containing 50 mM NaCl and 50 mM Tris−HCl, pH 8.0, adjusted with HCl), which served to elute unbound proteins. The target fusion proteins, bound to the column via their His-tags, were then eluted with an elution buffer (50 mM NaCl, 50 mM Tris−HCl, and 500 mM imidazole, pH 8.0, adjusted with HCl).

Elution fractions were analyzed via 12% SDS-PAGE followed by Coomassie Brilliant Blue G-250 staining to verify the protein purity. The Bradford protein assay (Sangon Biotech), benchmarked against BSA standards, was used to quantify the protein concentrations in the eluted fractions, enabling a precise determination of the yields for subsequent biochemical assays.

Activity Assays for ScGalK/ScGPUT Fusion Enzymes

To evaluate the catalytic function of the *Sc*GalK/*Sc*GPUT fusion enzymes, two sets of reactions were prepared for analysis using TLC. The first reaction mixture comprised 50 μL of D-xylose (1 mM), ATP (2 mM), UTP (3 mM), $MgCl_2$ (2 mM), and the reaction buffer (100 mM Tris−HCl, pH 7.5). The second set of reactions had a similar composition with the substitution of 1 mM D-xylose-1-phosphate in place of D-xylose. Both reactions included one of the eight varied fusion enzyme constructs and were incubated at 30 °C for an extensive period of 48 h to facilitate the synthesis of UDP-xylose. Various ratios of *Sc*GalK to *Sc*GPUT (1:1, 1:2, 1:3, 2:1, and 3:1) were tested based on their respective molarities.[10]

The enzymatic reactions were terminated by denaturing the samples at 95 °C for 5 min. The samples were then centrifuged at 20,000*g* for 5 min to remove any insoluble material. A volume of 1 μL from the clear supernatant of each sample was applied to silica gel 60 F254 TLC sheets (Supelco). The chromatographic separation was achieved with the mobile phase consisting of *n*-butanol, ethanol, and water in a volumetric ratio of 5:3:2, respectively.

To visualize the separated products, TLC sheets were developed using an orcinol staining solution prepared by dissolving 40 mg of orcinol monohydrate in 20 mL of 3.6 M sulfuric acid, followed by heating until the detection of spots.

Quantitative densitometry was conducted using ImageJ software to analyze the intensity of the UDP-xylose spots captured on the TLC plates.[23] The relative activity and expression level of each fusion enzyme were calculated by comparing the grayscale intensity values of each UDP-xylose spot to the highest intensity value recorded among the samples, enabling a comparative evaluation of the catalytic efficiency across the fusion enzyme variants. To determine the kinetic parameters of the linker 8 fusion enzymes and the unfused *Sc*GalK/*Sc*GPUT enzymes, various concentrations of D-xylose (ranging from 0.1 to 10 mM) were tested. The values for V_{max}, K_m, k_{cat}, and K_m/k_{cat} were calculated using nonlinear regression analysis with GraphPad Prism (version 9.5) software.

Mass Spectrometric Analysis of Reaction Products

The enzymatic products resulting from the activity of the *Sc*GalK/*Sc*GPUT fusion enzymes were analyzed through LC-ESI-MS by employing a Shimadzu LCMS 8040 system. The system configuration included an LC-30AD pump, featuring a low-pressure gradient mixing unit, and a SIL-30AC autosampler seamlessly integrated with an ESI mass detector. For the analysis, 5 μL of the clarified reaction supernatant was diluted with 10 μL of water and 35 μL of acetonitrile. A 10 μL aliquot of the resultant solution was introduced into the LC-ESI-MS for chromatographic separation.

https://doi.org/10.1021/jacsau.4c00288
JACS Au 2024, 4, 2557−2563

The separation was executed on a hydrophilic interaction liquid chromatography (HILIC) ethylene bridged hybrid (BEH) UPLC column (Waters Acquity glycan column, 1.7 μm particle size, 2.1 mm internal diameter × 150 mm length) maintained at 60 °C. With a solvent flow rate set at 0.5 mL/min, the mobile phase consisted of an ammonium formate buffer (50 mM, pH 4.5, referred to as solvent A) and acetonitrile (referred to as solvent B), initially mixed in a 5:95 (v/v) proportion. Over a linear gradient of 14.5 min, solvent B was raised from 5 to 60%, resulting in the elution of UDP-D-xylose at 11.6 min into the run.

Mass spectrometric data was collected in scan mode, covering a mass range from 150 to 700 m/z. This range was specifically chosen to target UDP-D-xylose, and the analysis was conducted using negative ion mode. The settings included a capillary voltage of −3.5 kV and a scan duration of 500 ms per cycle. The desolvation temperature was set to 250 °C, and a nitrogen gas flow rate was sustained at 900 L/h to ensure proper ionization of the analytes.

■ ASSOCIATED CONTENT

Supporting Information

The Supporting Information is available free of charge at https://pubs.acs.org/doi/10.1021/jacsau.4c00288.

Detailed descriptions and sequences of oligonucleotide primers used in this study; kinetic analyses of enzyme variants; and various figures illustrating experimental procedures and results, including SDS-PAGE analysis, thin-layer chromatography, and optimal conditions for enzymatic activity (PDF)

■ AUTHOR INFORMATION

Corresponding Authors

Li Liu − *Glycomics and Glycan Bioengineering Research Center (GGBRC), College of Food Science and Technology Nanjing Agricultural University, 210095 Nanjing, China;* orcid.org/0000-0002-2178-9237; Email: lichen.liu@njau.edu.cn

Josef Voglmeir − *Glycomics and Glycan Bioengineering Research Center (GGBRC), College of Food Science and Technology Nanjing Agricultural University, 210095 Nanjing, China;* orcid.org/0000-0002-4096-4926; Email: josef.voglmeir@njau.edu.cn

Authors

Jin-Da Zhuang − *Glycomics and Glycan Bioengineering Research Center (GGBRC), College of Food Science and Technology Nanjing Agricultural University, 210095 Nanjing, China*

Jin-Min Shi − *Glycomics and Glycan Bioengineering Research Center (GGBRC), College of Food Science and Technology Nanjing Agricultural University, 210095 Nanjing, China*

Chen-Cheng Hong − *Glycomics and Glycan Bioengineering Research Center (GGBRC), College of Food Science and Technology Nanjing Agricultural University, 210095 Nanjing, China*

Ting-Ting Wu − *Glycomics and Glycan Bioengineering Research Center (GGBRC), College of Food Science and Technology Nanjing Agricultural University, 210095 Nanjing, China*

Complete contact information is available at: https://pubs.acs.org/10.1021/jacsau.4c00288

Author Contributions

†J.-D.Z. and J.-M.S.: equal contribution. CRediT: **Jin-Da Zhuang** data curation, formal analysis, investigation, validation, visualization, writing-review & editing; **Jin-Min Shi** data curation, writing-original draft; **Chen-Cheng Hong** data curation; **Ting-Ting Wu** data curation.

Notes

The authors declare no competing financial interest.

■ REFERENCES

(1) Lee, T. V.; Sethi, M. K.; Leonardi, J.; Rana, N. A.; Buettner, F. F. R.; Haltiwanger, R. S.; Bakker, H.; Jafar-Nejad, H. Negative Regulation of Notch Signaling by Xylose. *PLoS Genet.* **2013**, *9* (6), No. e1003547.

(2) Yuan, Y.; Teng, Q.; Zhong, R.; Haghighat, M.; Richardson, E. A.; Ye, Z. H. Mutations of Arabidopsis TBL32 and TBL33 Affect Xylan Acetylation and Secondary Wall Deposition. *PLoS One* **2016**, *11* (1), No. e0146460.

(3) Puchner, C.; Eixelsberger, T.; Nidetzky, B.; Brecker, L. Binding Pattern of Intermediate UDP-4-Keto-Xylose to Human UDP-Xylose Synthase: Synthesis and STD NMR of Model Keto-Saccharides. *Carbohydr. Res.* **2017**, *437*, 50−58.

(4) Eixelsberger, T.; Weber, H.; Nidetzky, B. Probing of the Reaction Pathway of Human UDP-Xylose Synthase with Site-Directed Mutagenesis. *Carbohydr. Res.* **2015**, *416*, 1−6.

(5) Duan, X. C.; Lu, A. M.; Gu, B.; Cai, Z. P.; Ma, H. Y.; Wei, S.; Laborda, P.; Liu, L.; Voglmeir, J. Functional Characterization of the UDP-Xylose Biosynthesis Pathway in Rhodothermus Marinus. *Appl. Microbiol. Biotechnol.* **2015**, *99* (22), 9463−9472.

(6) Lowry, O. H.; Passonneau, J. V. Phosphoglucomutase Kinetics with the Phosphates of Fructose, Glucose, Mannose, Ribose, and Galactose. *J. Biol. Chem.* **1969**, *244* (3), 910−916.

(7) Albrecht, G. J.; Bass, S. T.; Seifert, L. L.; Hansen, R. G. Crystallization and Properties of Uridine Diphosphate Glucose Pyrophosphorylase from Liver. *J. Biol. Chem.* **1966**, *241* (12), 2968−2975.

(8) Tenhaken, R.; Thulke, O. Cloning of an Enzyme That Synthesizes a Key Nucleotide-Sugar Precursor of Hemicellulose Biosynthesis from Soybean: UDP-Glucose Dehydrogenase. *Plant Physiol.* **1996**, *112* (3), 1127−1134.

(9) Moriarity, J. L.; Hurt, K. J.; Resnick, A. C.; Storm, P. B.; Laroy, W.; Schnaar, R. L.; Snyder, S. H. UDP-Glucuronate Decarboxylase, a Key Enzyme in Proteoglycan Synthesis: Cloning, Characterization, and Localization. *J. Biol. Chem.* **2002**, *277* (19), 16968−16975.

(10) Shi, J. M.; Wu, T. T.; Zhou, H.; Zhang, Y. Y.; Liu, L.; Widmalm, G.; Voglmeir, J. Substrate Promiscuities of a Bacterial Galactokinase and a Glucose-1-Phosphate Uridyltransferase Enable Xylose Salvaging. *Green Chem.* **2022**, *24*, 3717−3722.

(11) Coyne, M. J.; Reinap, B.; Lee, M. M.; Comstock, L. E. Human Symbionts Use a Host-like Pathway for Surface Fucosylation. *Science.* **2005**, *307* (5716), 1778−1781.

(12) Gangl, R.; Behmüller, R.; Tenhaken, R. Molecular Cloning of a Novel Glucuronokinase/Putative Pyrophosphorylase from Zebrafish Acting in an UDP-Glucuronic Acid Salvage Pathway. *PLoS One* **2014**, *9* (2), No. e89690.

(13) Zhai, Y.; Liang, M.; Fang, J.; Wang, X.; Guan, W.; Liu, X. wei; Wang, P.; Wang, F. NahK/GlmU Fusion Enzyme: Characterization and One-Step Enzymatic Synthesis of UDP-N-Acetylglucosamine. *Biotechnol. Lett.* **2012**, *34* (7), 1321−1326.

(14) Quin, M. B.; Wallin, K. K.; Zhang, G.; Schmidt-Dannert, C. Spatial Organization of Multi-Enzyme Biocatalytic Cascades. *Org. Biomol. Chem.* **2017**, *15* (20), 4260−4271.

(15) Han, Y.-Y.; Yue, H.-Y.; Zhang, X.-Y.; Lyu, Y.-M.; Liu, L.; Voglmeir, J. Construction and Evaluation of Peptide-Linked Lactobacillus Brevis β-Galactosidase Heterodimers. *Protein Pept. Lett.* **2021**, *28* (2), 221−228.

(16) Chen, X.; Zaro, J. L.; Shen, W. C. Fusion protein linkers: property, design and functionality. *Adv. Drug Delivery Rev.* **2013**, *65* (10), 1357−1369.
(17) Chen, H. Y.; Chen, Z.; Wu, B. G.; Ullah, J.; Zhang, T. X.; Jia, J. R.; Wang, H. C.; Tan, T. W. Influences of Various Peptide Linkers on the Thermotoga maritima MSB8 Nitrilase Displayed on the Spore Surface of Bacillus subtilis. *J. Mol. Microb. Biotechnol.* **2017**, *27*, 64−71.
(18) Argos, P. An investigation of Oligopeptides Linking Domains in Protein Tertiary Structures and Possible Candidates for General Gene Fusion. *J. Mol. Biol.* **1990**, *211* (4), 943−958.
(19) Crowe, S. A.; Zhao, X.; Gan, F.; Chen, X.; Hudson, G. A.; Astolfi, M. C. T.; Scheller, H. V.; Liu, Y.; Keasling, J. D. Engineered *Saccharomyces Cerevisiae* as a Biosynthetic Platform of Nucleotide Sugars. *ACS Synth. Biol.* **2024**, *13*, 1215−1224.
(20) Reed, M. C.; Lieb, A.; Nijhout, H. F. The Biological Significance of Substrate Inhibition: A Mechanism with Diverse Functions. *BioEssays.* **2010**, *32* (5), 422−429.
(21) Lapp, D.; Elbein, A. D. Purification and Properties of the Adenosine Diphosphate-Glucose and Uridine Diphosphate-Glucose Pyrophosphorylases of Mycobacterium Smegmatis: Inhibition and Activation of the Adenosine Diphosphate-Glucose Pyrophosphorylase. *J. Bacteriol.* **1972**, *112* (1), 327−336.
(22) Chen, X.; Fang, J.; Zhang, J.; Liu, Z.; Shao, J.; Kowal, P.; Andreana, P.; Wang, P. G. Sugar Nucleotide Regeneration Beads (Superbeads): a Versatile Tool for the Practical Pynthesis of Oligosaccharides. *J. Am. Chem. Soc.* **2001**, *123* (9), 2081−2082.
(23) Schneider, C. A.; Rasband, W. S.; Eliceiri, K. W. NIH Image to ImageJ: 25 Years of Image Analysis. *Nat. Methods* **2012**, *9* (7), 671−675.

https://doi.org/10.1021/jacsau.4c00288
JACS Au 2024, 4, 2557−2563